A RANS-based surrogate model for simulating wind turbine interaction

A RANS-based surrogate model for simulating wind turbine interaction

J. Criado Risco, M. P. van der Laan, M. M. Pedersen, A. Meyer Forsting, P.-E. Réthoré

Technical University of Denmark, Frederiksborgvej 399, 4000 Roskilde, Denmark

E-mail: jcrri@dtu.dk

Abstract. A new wake surrogate model based on Reynolds-averaged Navier-Stokes (RANS) single rotor simulations is presented. The model relies on a series of three-dimensional pre-calculated deficit and added turbulence intensity flow fields, stored in a look-up table (LUT) as a function of the thrust coefficient and the ambient turbulence intensity. For any combination of these parameters, the flow around a wind turbine can be predicted by linearly interpolating within the look-up table. Furthermore, the resulting three-dimensional flow fields from different turbine sources can be superposed linearly to calculate the total wind farm flow. The model is implemented in PyWake and benchmarked against other, commonly employed engineering wake models, namely the Gaussian-Bastankhah, the N. O. Jensen and the Zong models, where RANS wind farm simulations are used as reference. In both full and partial wake cases, the surrogate model achieves a higher accuracy than any other model. Besides providing an accuracy comparable to a full RANS solution, the model can compute a flow case in the order of 1 s on a single processor. The main disadvantage is that the generation of the look-up table is time consuming, computationally expensive and can be memory demanding (especially if more inputs, such as the yaw misalignment angle, stability, etc. are added). Nevertheless, generating the LUT only has to be done once per wind turbine type.

1. Introduction

The annual energy production (AEP) is an essential parameter when it comes to assess the profitability of a wind energy project. The maximization of AEP is typically used as an objective function or a component of the cost function in wind farm layout optimization problems [1, 2, 3]. The AEP calculation requires modelling the interaction between atmospheric flow and wind turbines in order to quantify wake losses. Complex and computationally heavy numerical models can characterize the interaction between flow and wind turbines with a high level of fidelity. These are usually based on Computational Fluid Dynamics (CFD). The main drawback of this method is the excessive use of computational resources even for relatively small wind farm simulations. Although high fidelity is preferred in general, the use of CFD models in an optimization framework becomes impractical given the amount of time and computational resources needed to run a single flow case. Typically, an AEP evaluation requires computing in the order of 10^4 flow cases. Therefore more simplified and efficient models are needed for this application. Analytical models rely on mathematical expressions that are based on calibrated parameters and can resolve the flow in a matter of seconds. These models provide efficiency and fast solutions, making them suitable for optimization purposes. In turn, they do not capture

as much physics as CFD models, achieving lower fidelity in power estimations. The Jensen [4] model—one of the most popular wake deficit models—represents the wake behind a wind turbine by means of top-hat profile and a linear wake expansion factor. Another approach commonly used within academia is the one proposed by Bastankhah et al. [5]. It is based on mass and momentum conservation and assumes a Gaussian wake deficit distribution, but retains the linear wake expansion behaviour of the Jensen approach. Extensions to the Bastankhah were proposed by multiple authors in the meantime: Niayifar et al. [6] added a dependency of the wake expansion factor to the local turbulence intensity (TI) using LES simulations—later modified by Carbajo-Fuertes et al. [7] using lidar measurements—and Zong et al. [8] additionally tried to incorporate a more realistic representation of the near-wake by incorporating Vermeulen's expression for the near wake length and adding the gradual growth of the thrust force by Shapiro et al.; Larsen [9] proposed an analytical solution of the wake assuming symmetric flow fields and uniform inflow, in which the expansion was modelled by an empirical function dependent on the rotor diameter, thrust and turbulence intensity. Nygaard et al. [10] recently introduced the TurboPark model, which considers the ambient atmospheric turbulence and the turbulence generated in the wake itself, improving the representation of the wake recovery. Strategies like linearising the Navier Stokes equations have also been used to reduce the fidelity gap between CFD and analytical models while still providing a fast way of solving the flow. An example of this is Fuga, which is based on a series of look-up tables, some general and some turbine specific, that allow to construct the velocity fields around a single or multiple turbines [11].

Besides wind speed deficits, the turbulence intensity is another variable that impacts the wake and fatigue loads of downstream wind turbines. Different analytical models can also be found in the literature for its calculation. Crespo et al. [12] developed an analytical expression for the estimation of the turbulent kinetic energy and its dissipation rate based on CFD results; Larsen et al. [13] proposed a dynamic wake meandering model combining the effect of atmospheric turbulence, added wake turbulence and the intermittent contribution caused by wake meandering. Frandsen developed another analytical model that served as the base for the IEC61400-1 standard [14], which estimates a term that is added to the representative ambient turbulence standard deviation. However, this model was developed to estimate loads and is not suitable to capture the TI effect on the wake recovery. More recently, the developments of turbulence analytical models include additional functions or terms for correction. Qian and Ishihara [15] proposed a new multi-wake model accounting for the local effective rotor inflow, where turbulence from different turbines is added using Linear Superposition of Square with a correction term that considers wake mixing. Li et al. [16] proposed a novel three-dimensional analytical model for the added turbulence intensity considering the ground effect and a new correction function to superpose the turbulence from different wakes. Tian et al. [17] developed two analytical models, the first is one-dimensional and estimates the wake width and maximum wake turbulence level at any stream-wise position, and the second is three-dimensional and is based on the first one, being able to estimate the turbulence intensity in the wake.

An alternative approach is to build data-driven based models, also known as surrogates, which can capture more physics while avoiding the CFD large computational efforts. An example of this is introduced by Göçmen and Giebel in [18], where a neural network is trained to predict wind speeds at a downstream wind turbine, outperforming engineering models specifically calibrated for the given wind farm. In [19], L. Wang et al. create a wake model using three neural network algorithms, based on a database generated with actuator disc simulations. Out of the three algorithms, the best one is able to estimate the deficits with less than 6 % of error in the far wake region. Another example is described by Schmidt and Stoevesandt [20], where a RANS solver is used to pre-compute the deficit fields of a single wind turbine for a range of inflow wind speeds, storing all the results in a database. The deficit for flow cases different from those simulated, can be interpolated from the database, and superimposed to predict the total deficits

within a wind farm. Their proof of concept demonstrated that it is possible to use this approach to model multiple wakes within farms, although their results showed that their model lacked some accuracy, as overlapping deficits were not completely reflecting the behaviour of a wind farm CFD simulation.

As Schmidt and Stoevesandt suggested in their conclusions, their method could be extended to more dimensions, for instance, including TI as a local inflow parameter. Furthermore, according to scaling laws, given that wind turbines operate under a sufficiently high Reynolds number—as they do in full-scale wind farms—and if neutral atmospheric stability is assumed, the resulting deficit fields from a wind farm simulation will only depend on three parameters: the rotor-averaged turbine thrust coefficient, C_T, the ambient turbulence intensity, TI_∞, and the diameter-to-hub height ratio, D/z_H [21]. This means that the deficit fields can be normalized with the inflow wind speed to be stored in the LUT only as a function of the aforementioned parameters, and then re-scaled using the local effective wind speed for any turbine within a wind farm.

The purpose of this work is to model the wind speed deficits within a wind farm with high accuracy using a database of RANS single rotor simulations. This is similar to the approach by Schmidt and Stoevesandt [20], where the wake deficit is no longer wind speed but instead thrust coefficient dependent, and our database includes an additional dependence on ambient turbulence intensity. The outcome of this work is a RANS-based wake surrogate model, based on linear interpolation within a multidimensional look-up table (LUT), that can accurately compute wake deficits and turbulence within wind farms at limited computational cost.

2. Methodology

The LUT and wind farm reference data are created by performing RANS simulations within PyWakeEllipSys v3.0[22], a plug-in to PyWake [23] developed at DTU Wind & Energy Systems that uses a Python interface to the general purpose CFD solver EllipSys3D [24, 25] and associated in-house tools. A brief description of the models' setup is provided.

2.1. PyWakeEllipSys

The wind turbines are modelled as actuator discs (AD), that are coupled to the flow domain via an intersectional grid as described by Réthoré et al. [26] and Troldborg et al. [27]. The polar grid is discretised by 64×64 radial and azimuthal cells, respectively. The forces over the AD polar grid are calculated from the local cell velocity in combination with analytic formulations for the normal and tangential radial force distributions, as described by Sørensen et al. [28]. This method only requires the wind turbine's power, thrust and tip speed ratio curves and its diameter for scaling the forces; here we have chosen to use the DTU10MW reference wind turbine [29] operating curves and dimensions.

A Cartesian grid is used to model a site with an uniform roughness. A fine region with uniform grid spacing encompasses the AD with an extension of $4D$ upstream, $20D$ downstream, and $2.5D$ to each of the lateral directions of the rotor. The cell size in this region is $D/12$. From the inner region, the mesh grows hyperbolically towards the domain boundaries, which are set to $500D$ from each face of the inner domain. In the vertical, the mesh expands exponentially from a wall cell height of $2.8 \times 10^{-3}D$ towards the upper lid at $25D$. The mesh for the wind farm simulations identical, except that the uniformly spaced, inner grid is extended to end $20D$ downstream of the rearmost turbine.

The steady-state inflow model is characterised by a logarithmic wind profile coupled with a turbulence model based on the k-ε-f_P model [30]. This turbulence model adds a scalar term f_P that improves the interaction between the wind turbine wakes and the neutral atmospheric surface layer (ASL). The inflow profile is fully determined by selecting a wind speed and TI at a reference height. Throughout this work, the reference height is set at hub height, z_H, indicated

by the subscript H. Therefore, we use $U_H = U_\infty(z = z_H)$ and $TI_H = TI_\infty(z = z_H)$ to refer to the respective inflow quantities at hub height (undisturbed, far in front of the most upstream wind turbine). It is in fact TI_H that determines the roughness length, z_0, of the log profile in this turbulence model as:

$$TI_H = \frac{\kappa\sqrt{\frac{2}{3}}}{C_\mu^{\frac{1}{4}} \ln\left(\frac{z_H+z_0}{z_0}\right)} \tag{1}$$

where C_μ and κ are model constants (refer to [30]). Therefore here higher TI will lead to greater shear.

To enable capturing thrust and TI variations within wind farms accurately, a wide parameter space was sampled to generate the single-turbine LUT, i.e. $C_T = \{0.1, 0.2, ..., 1.0\}$ and $TI_H = \{0.05, 0.1, 0.2, 0.3\}$. Therefore a total of 40 single-rotor RANS simulations were run.

The output of a PyWakeEllipSys simulation can be saved as a netCDF file (network Common Data Form). This file format allows storing multidimensional data as a function of different coordinates. The LUT stores: (1) the normalised deficits in the stream wise direction, $\Delta U = 1 - U/U_\infty$, where U represents the velocity component in the stream-wise direction; and (2) the added turbulence intensity, $\Delta TI = (\sqrt{\frac{2}{3}k_\infty} - \sqrt{\frac{2}{3}k})/U_\infty$, where k represents the turbulent kinetic energy. The dimensions of the LUT are the spatial coordinates x, y, z, and the parameters TI_H and C_T. The generated LUT netCDF file size is about 2.4 GB.

2.2. Implementation in PyWake

The surrogate model is implemented in PyWake [23, 31], DTU Wind's open-source tool for wind farm flow and AEP calculations. PyWake is heavily vectorised and is thus extremely fast. Another strength is its modularity, which provides complete flexibility in how to combine different sub-components modelling deficits, blockage, turbulence, deflection, superposition, and more.

Figure 1 illustrates an example of how the deficits are retrieved from the LUT and superimposed in PyWake, also comparing them to RANS wind farm simulations. The upper row shows a schematic of two aligned turbines in a farm for which wind speed profiles are to be determined far up- and downstream ($x_1 = 12D$) indicated by the vertical lines. Their colours should enable differentiating between the profiles' location. The four plots in the lower row of Fig. 1 graphically describe the LUT superposition process adopted within PyWake. The leftmost plot shows the identical inflow profiles, set through U_H and TI_H, of the RANS wind farm simulations (yellow) and PyWake (grey) present far upstream of the farm. All subsequent plots compare profiles downstream of the the two turbines, $12D$ and $5D$ from the first and second rotor, respectively. The turbine operating conditions are determined by extracting the effective wind speed, $\hat{U}$, and $\hat{TI}$ from the flow field at the respective rotor centres. As the second turbine is operating in the wake of the first, it is operating in lower wind speed (higher C_T) and higher TI. These operating conditions are then used in combination with the relative spatial coordinates of the profile where the deficit is to be computed, to interpolate the normalised deficit, ΔU, from the LUT. As shown in the second plot, the normalised deficits from the respective LUT interpolations are re-scaled by the respective effective wind speed, $\hat{U}$, and summed (linear superposition) to arrive at the total wind speed deficit. Notice here that the deficit from the first rotor (blue line) exceeds that of the second (red line) for $z > 2 \cdot z_H$, as the shear changes with the TI_H as discussed in Sect. 2.1. Without shear the total deficit could simply be subtracted from the inflow hub-height wind speed as shown in the third plot. However, good agreement with the RANS wind farm simulations are only achieved when scaling the deficit according to the shear profile and subtracting it from the inflow profile as shown in the rightmost plot. A similar approach is followed for determining the TI, only that the total

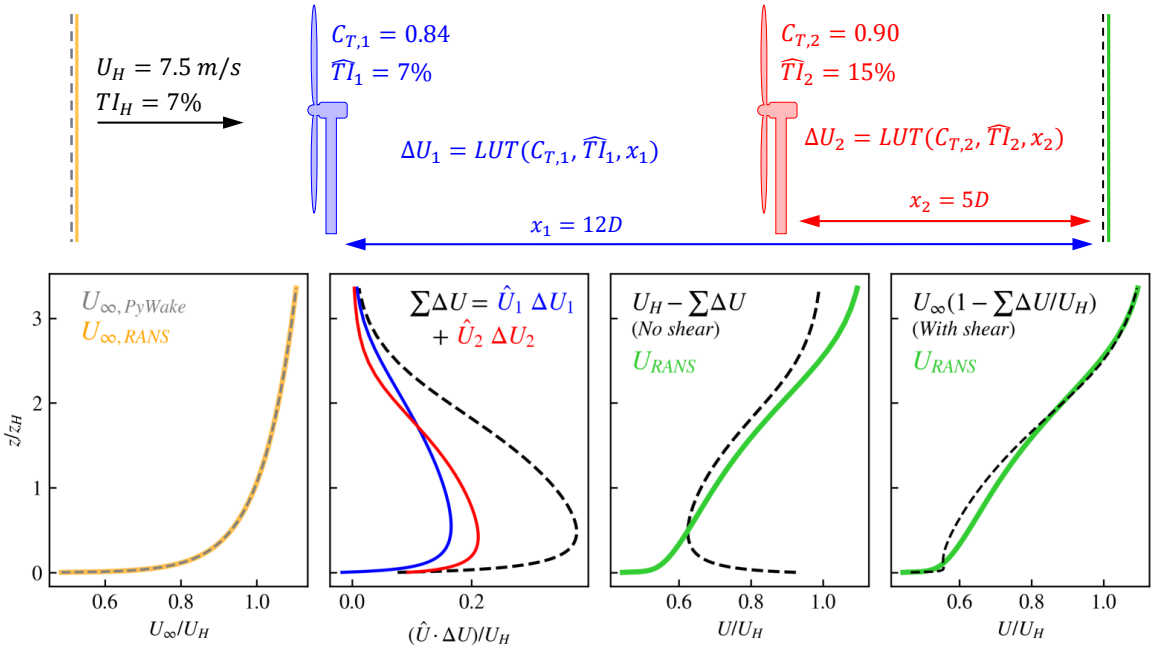

Figure 1. Graphical representation of the LUT implementation in PyWake, and comparison to RANS wind farm simulations for a vertical profile downstream of two aligned turbines.

TI is computed by summing the added TI contributions from each turbine and adding them to TI_H.

Finally, here the power computation in PyWake followed the approach taken for the RANS wind farm simulations (see [32] for details).

3. Superposition study

A superposition study is conducted to investigate the most suitable technique for combining the LUT predictions in wind farms and compared against full RANS simulations. Our LUTs contain added TI and deficit fields, therefore the superposition problem needs to be studied independently for each of them.

A wind farm consisting of four aligned wind turbines is defined and parameterised to generate different test cases; four rotors, as then the asymptotic limits for the deficits and added TI are approximately reached. As inferred by a previous study [33], we can expect larger LUT prediction errors for low ambient TI and high thrust coefficients, thus inflow conditions and turbine spacing are expected to influence prediction accuracy. Based on this, three different cases are defined to study the effect of turbine spacing, S, ambient TI and thrust coefficient (determined through the inflow wind speed):

- Case 1: $TI_H = 5\%$, $U_H = 8$ m/s and $S = 4D$;
- Case 2: $TI_H = 5\%$, $U_H = 8$ m/s and $S = 7D$;
- Case 3: $TI_H = 12\%$, $U_H = 11.7$ m/s and $S = 4D$.

3.1. Added turbulence intensity superposition

The superposition of TI fields from different wind turbine sources is a topic not yet fully understood. According to Machefaux et al. [34], most commonly used superposition techniques rely on simple mathematical rules that are not justified by any physical means. Based on

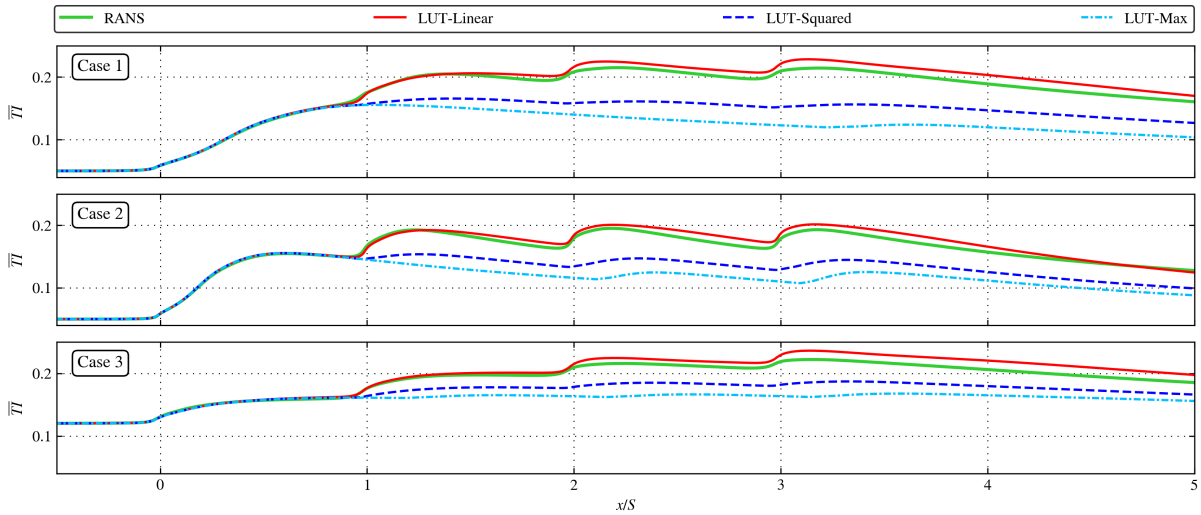

Figure 2. Rotor-integrated TI resulting from applying different added TI superposition techniques and their comparison with RANS wind farm simulations.

the techniques found in the literature for deficit superposition, we investigated the following methods, where ΔTI_n represents the added TI generated by the n^{th} wind turbine:

Superposition technique	Mathematical rule
Linear sum	$TI_\infty + \Delta TI_1 + \Delta TI_2 + ... + \Delta TI_n$
Squared sum	$TI_\infty + \sqrt{\Delta TI_1^2 + \Delta TI_2^2 + ... + \Delta TI_n^2}$
Max sum	$TI_\infty + \max(\Delta TI_1, \Delta TI_2, ..., \Delta TI_n)$

Figure 2 illustrates the rotor-integrated TI variation ($\overline{\bullet} = \int_A \bullet \, dA/(\pi R^2)$) with downstream distance for the different superposition models, with RANS wind farm results as reference. Table 1 summarises the averaged and maximum relative differences with respect to the reference. The results show good agreement when using linear summation for all the three flow cases, although TI is slightly overestimated. Both the squared sum and the max sum underestimate the turbulence intensity downstream, performing significantly worse. The second flow case is the one with lower errors, as expected due to the increased spacing between turbines. The third flow case shows lower errors with respect to the first case, as higher ambient TI and wind speeds (lower thrust coefficient) are more favorable conditions for using LUT predictions, as described in [33].

3.2. Velocity deficits superposition

In contrast to TI superposition, wind speed deficit superposition in wind farm wakes has been a topic of research for many years. Lissaman used linear superposition to model overlapping deficit fields from different turbine sources [35]. Crespo et al. questioned later in [36] the validity of linear summation, as negative velocities could occur when large perturbations from many upstream wakes overlapped. Katic et al. [37] suggested the application of quadratic summation of deficits from different turbine sources. Their assumption was based on results validated with experimental data, where squared superposition achieved better performance. Larsen et

Superposition	Avg. relative difference			Max. relative difference		
	Case 1	Case 2	Case 3	Case 1	Case 2	Case 3
Linear sum	-0.4	-0.3	-0.6	-1.5	-1.2	-1.5
Squared sum	3	2.6	1.6	6	5.5	3.8
Max sum	4.5	3.8	2.5	9.4	8.3	6

Table 1. TI superposition results. Averaged and maximum relative differences with respect to RANS wind farm simulations.

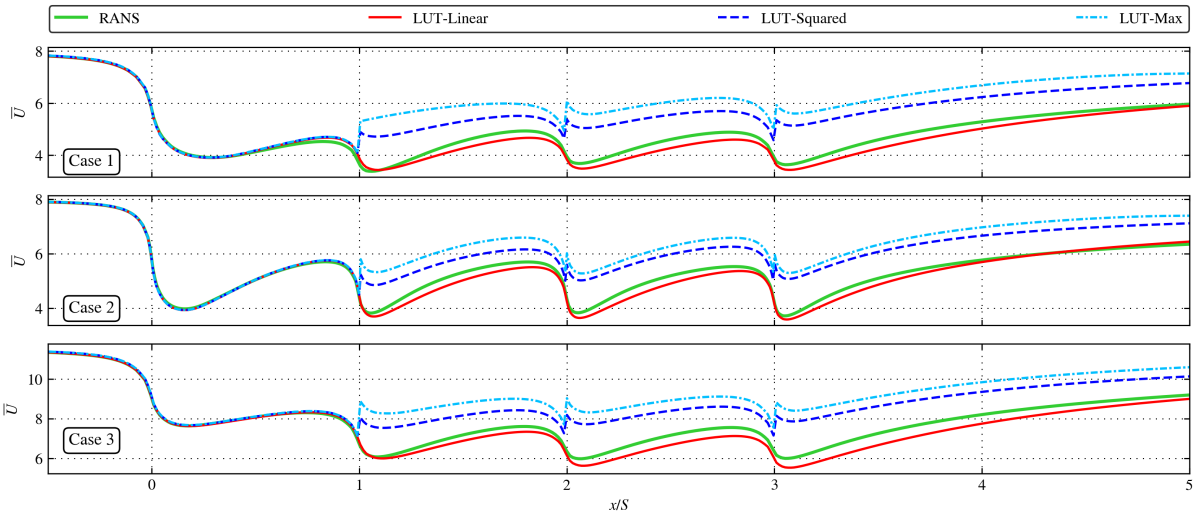

Figure 3. Rotor-integrated wind speed resulting from applying different deficit superposition techniques and their comparison with RANS wind farm simulations.

al. sustained that the deficit would be determined by the dominant wake [13], therefore they argued that the local deficit should be based on the maximum deficit of all interacting wakes.

Based on these approaches found in the literature, the performance of the LUT predictions is investigated by applying the superposition techniques "linear sum", "squared sum" and "maximum sum" available within PyWake for estimating the combined deficit fields, as described in Table 1 (using ΔU rather than ΔTI). Here the added TI fields are linearly superimposed to determine the effective TI at the turbines, $\hat{TI}$, as it provided more accurate results.

Figure 3 illustrates the rotor-integrated streamwise wind speed variation. Table 2 summarises the respective average and maximum relative differences. Once again linear deficit summation provides more accurate results when compared to the RANS wind farm reference, though underestimating the wind speed in the wakes of the last two turbines. Both the squared sum and the max sum overestimate the wind speeds when two or more wakes merge, leading to larger errors. Results for the second case indicate that the increased spacing between turbines has a positive impact, since the relative differences are slightly reduced. In the third flow case, as opposed to what was observed in T superposition, the higher inflow wind speed and ambient TI do not result in lower relative differences. This is due the thrust coefficients used to interpolate are further from the values included in the LUT. For instance, the fourth wind turbine gives a thrust coefficient of 0.92 in the first flow case, compared to a thrust coefficient of 0.83 in the third flow case.

Superposition	Avg. relative difference [%]			Max. relative difference [%]		
	Case 1	Case 2	Case 3	Case 1	Case 2	Case 3
Linear sum	0.6	0.7	1.5	2.9	2.8	5.1
Squared sum	-5.7	-5.2	-6.8	-13.6	-12.5	-17
Max sum	-8.1	-7.2	-10	-18.5	-15.6	-23

Table 2. Deficit superposition results. Average and maximum relative differences with respect to RANS wind farm simulations.

4. LUT benchmarking against engineering wake models

In this section, the LUT model is compared against RANS and other engineering models found in literature. Linear summation is used for the superposition of both TI and deficit fields, as it achieved better results in the superposition study. The section is divided in two parts: first, a flow case with ten wind turbines in a row is analysed. For this, the rotor-integrated wind speeds are compared. In addition, a case with three staggered wind turbines is defined, and wind speeds are compared over a horizontal plane at hub height.

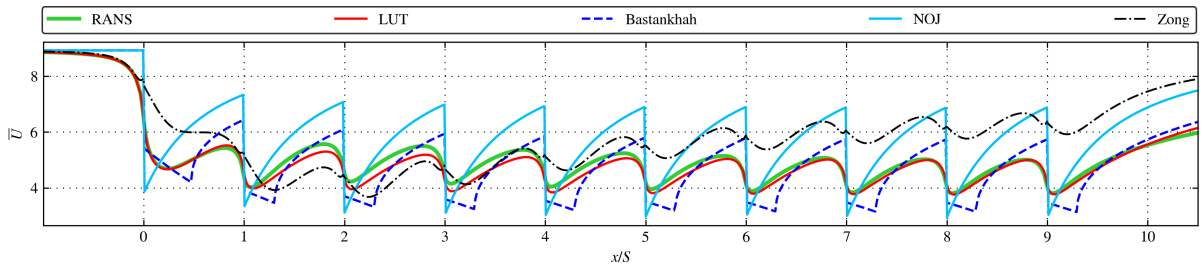

Figure 4. Comparison of rotor-integrated streamwise wind speed variation for ten aligned turbines predicted by RANS simulations, PyWake-LUT and other engineering models.

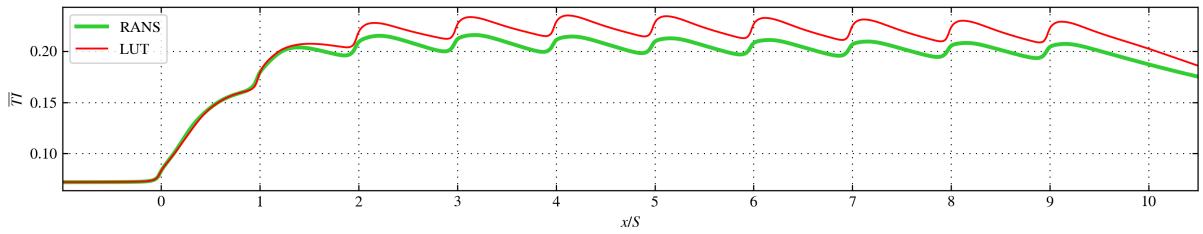

Figure 5. Comparison of rotor-integrated streamwise TI variation for ten aligned turbines predicted by RANS simulations and PyWake-LUT.

4.1. Case 1: aligned wind turbines

A wind farm consisting of ten aligned turbines and separated by a spacing of $4D$ is investigated here. The hub height inflow wind speed is set to 9 m/s and TI_H to 7.2%. Besides the LUT model described in this work, other wake models found in literature are used to compute the deficits downstream and compared to RANS simulations: the Gaussian-Bastankhah model [5], the N.O. Jensen model [4], and the Zong model [8]. The Zong model is additionally setup with a blockage

model (Self-Similarity deficit 2020, based on [38]) and a turbulence model (Steen Frandsen model as in [14]). The Bastankhah and Jensen models both use "square sum" for deficit superposition, while the wind farm model with the Zong deficit model uses linear summation similar to the LUT.

Figure 4 illustrates the resulting rotor-integrated wind speed for each of the wake models as a function of the downstream distance. Additionally, Figure 5 compares the rotor-integrated TI between the LUT and RANS. The LUT comes closest to the RANS predictions, with a mean difference of +1.3% and maximum relative difference of +4.2% in the near wake of the third wind turbine.

Neither the Bastankhah nor the Jensen model are set-up to consider TI variations along the wind farm nor are they accounting for blockage effects. The wake expansion values are set to 0.038 for the Bastankhah and 0.1 for the Jensen. Whereas the Jensen model overestimates the wind speeds significantly, the Gaussian-Bastankhah shows lower variations with respect to RANS. These differences are larger at the rotors, reaching maximum values of -25.2% for the Bastankhah (most upstream rotor) and -31.2% for the Jensen (most downstream rotor).

Lastly, the Zong model setup achieves a close representation of the RANS simulations up to the fifth wind turbine ($x < -4D$), but then the error increases as the turbulence model does not correctly capture the variations within the wind farm. The maximum relative difference is reached at the last rotor, with a value of -26.6%.

In terms of wind farm power, the RANS simulations predict a production of 18.9 MW for the whole wind farm, whereas the LUT model estimates 19.4 MW (+2.8%). The wake engineering models estimate a wind farm power of: 11.18 MW using the Bastankhah set-up (-40.7%), 26.9 MW with Jensen (+42.2%) and 21.2 MW by Zong (+12%).

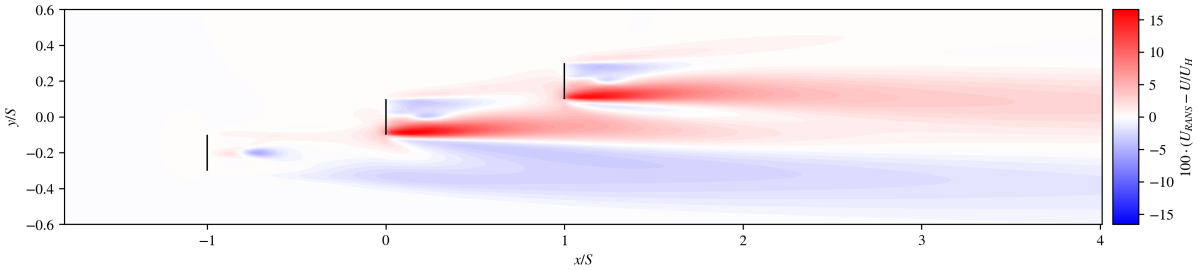

Figure 6. Relative difference between stream-wise wind speeds in a horizontal plane defined at hub height. The black lines represent the rotors as seen from above.

4.2. Case 2: staggered wind turbines

A wind farm consisting of three wind turbines with $5D$ streamwise and $1D$ lateral spacing is considered. A flow case is presented where the inflow wind speed at the hub height is set to 9 m/s and the TI to 7.2%. The purpose of this test case is to study the performance of the LUT approach in partial wake conditions.

Figure 6 presents the difference in streamwise wind speed between RANS wind farm simulations and LUT-based predictions. Differences are normalised by the hub height inflow wind speed. The LUT achieves a good agreement with RANS. Maximum differences around +15% are shown in the areas with partial wakes. This means that the wind speeds are slightly underestimated in the red areas. The wind farm power production is 14 MW for the RANS simulations, whereas the LUT predicts 13.6 MW (-3.2%).

5. Conclusions

A new wake surrogate model based on RANS single rotor simulations is presented. The model relies on a series of three-dimensional pre-calculated deficit and added turbulence intensity flow fields that are stored in a Look-up table (LUT) as a function of two fundamental parameters: the thrust coefficient and the ambient turbulence intensity, and of the spatial coordinates, x, y and z. For a given wind turbine, the parameters are estimated at its rotor and then used to interpolate linearly in the LUT. When several wind turbine sources coexist, the resulting three-dimensional flow fields can be superimposed to calculate the total wind farm flow. A superposition study reveals that the linear summation of both, the added turbulence intensity and the deficits, is most appropriate.

The RANS-based LUT is implemented in PyWake and benchmarked against other, common analytical wake models using RANS simulations as reference. A case with ten aligned wind turbines, separated by four rotor diameters in the streamwise direction, is used to prove that the LUT can accurately predict wind farm flows, achieving a higher accuracy than any of the other benchmarked engineering models. It presented a mean relative difference of +1.3% and a maximum relative difference of +4.2% with respect to the RANS simulations. Additionally, a case with partial wakes shows a good agreement with RANS predicted wind speeds at hub height level, with a maximum relative difference of +15% in partial wake areas. Power differences are in the order of ±3% between RANS and the LUT.

Using the LUT model, PyWake predicts AEP and far-wake flow fields within a few percent of full-fledged RANS CFD simulations, whilst running in the order of seconds on a single core. Therefore it presents a cheap alternative for predicting wind farm AEP. A drawback of the LUT is that its generation requires a high initial computational effort, but this has to be done only once. In addition, the LUT model can become memory-demanding as the size of the LUT increases (depends on the number of RANS single rotor simulations stored). However, this can be alleviated by removing the near-rotor region—unnecessary in wind farm AEP estimation—and only keeping height levels in which turbines are present or by simply just storing deficits at hub height. Without significant impact on accuracy, memory consumption following these measures can reduced by more than 99%. Another approach is to substitute the LUT by a neural network which is part of ongoing work [39].

References

[1] Grady S, Hussaini M and Abdullah M 2005 *Renewable Energy* **30** 259–270 ISSN 0960-1481
[2] Reddy S R 2021 *Renewable Energy* **165** 162–173 ISSN 0960-1481
[3] Pollini N 2022 *Renewable Energy* **195** 1015–1027 ISSN 0960-1481
[4] Jensen N O 1983 A note on wind generator interaction
[5] Bastankhah M and Porté-Agel F 2014 *Renewable Energy* **70** 116–123 ISSN 09601481
[6] Niayifar A and Porté-Agel F 2016 *Energies* **9** 741
[7] Carbajo Fuertes F, Markfort C D and Porté-Agel F 2018 *Remote Sensing* **10** ISSN 2072-4292
[8] Zong H and Porté-Agel F 2020 *Journal of Fluid Mechanics* **889** A8
[9] Larsen G 2009 *A simple stationary semi-analytical wake model* (*Denmark. Forskningscenter Risoe. Risoe-R* no 1713(EN)) (Risø National Laboratory for Sustainable Energy, Technical University of Denmark)
[10] Nygaard N G, Steen S T, Poulsen L and Pedersen J G 2020 *Journal of Physics: Conference Series* **1618** 062072
[11] Ott S, Berg J and Nielsen M 2011 *"Linearised CFD Models for Wakes"* 1772(EN) (Danmarks Tekniske Universitet, Risø Nationallaboratoriet for Bæredygtig Energi) ISBN 978-87-550-3892-9
[12] Crespo A and Hernández J 1996 *Journal of Wind Engineering and Industrial Aerodynamics* **61**(1) 71–85 ISSN 01676105
[13] Larsen G, Madsen H, Thomsen K and Larsen T 2008 *Wind Energy* **11** 377 – 395
[14] 2017 Iec 61400-1 Standard International Electrotechnical Commission
[15] Qian G and Ishihara T 2019 Prediction of flow field in wind farm using a new multiple wake model
[16] Li L, Huang Z, Ge M and Zhang Q 2022 *Energy* **238** 121806 ISSN 0360-5442
[17] Tian L, Song Y, Xiao P, Zhao N, Shen W and Zhu C 2022 *Renewable Energy* **189** 762–776

[18] Göçmen T and Giebel G 2018 *Journal of Physics: Conference Series* **1037** 072002
[19] Wang L, Xie J, Luo W, Wang Z, Zhang B, Chen M and Tan A C 2022 *Sustainable Energy Technologies and Assessments* **53** 102499 ISSN 2213-1388
[20] Schmidt J and Stoevesandt B 2014 Wind farm layout optimization with wakes from fluid dynamics simulations
[21] van der Laan M, Andersen S, Kelly M and Baungaard M 2020 *Journal of Physics: Conference Series* **1618** 062018
[22] DTU Wind and Energy Systems 2023 PyWakeEllipSys v3.0 `https://topfarm.pages.windenergy.dtu.dk/cuttingedge/pywake/pywake_ellipsys/`
[23] Pedersen M M, Forsting A M, Riva R, Romàn L A A, Risco J C, Friis-Møller M, Rodrigues R V, Quick J, Christiansen J P S and Réthoré P E 2022
[24] Michelsen J A 1992 General rights basis3d-a platform for development of multiblock pde solvers-release
[25] Sørensen N N 1995 General purpose flow solver applied to flow over hills. risø national laboratory
[26] Réthoré P E, Laan P V D, Troldborg N, Zahle F and Sørensen N N 2014 *Wind Energy* **17**(6) 919–937 ISSN 10991824
[27] Troldborg N, Sørensen N N, Réthoré P E and van der Laan M P 2015 *Computers and Fluids* **119** 197–203 ISSN 00457930
[28] Sørensen J N, Nilsson K, Ivanell S, Asmuth H and Mikkelsen R F 2020 *Renewable Energy* **147** 2259–2271 ISSN 18790682
[29] Bak C and *et al* 2013 The DTU 10-MW reference wind turbine
[30] van der Laan M P, Sørensen N N, Réthoré P E, Mann J, Kelly M C, Troldborg N, Schepers J G and Machefaux E 2015 *Wind Energy* **18** 889–907
[31] DTU Wind and Energy Systems 2022 Pywake `https://gitlab.windenergy.dtu.dk/TOPFARM/PyWake`, commit 03e6f425fe622809edb8f0a292671382e5342bff
[32] van der Laan M P, Sørensen N N, Réthoré P E, Mann J, Kelly M C and Troldborg N 2015 *Wind Energy* **18**(12) 2223–2240 ISSN 10991824
[33] Risco J C, van der Laan P, Mølgaard M P and Réthoré P E 2021 "A CFD surrogate model for annual energy production calculations of wind farms".
[34] Machefaux E, Larsen G C and Leon J P M 2015 *Journal of Physics: Conference Series* **625** 012037
[35] Lissaman P 1979 *Energy effectiveness of arbitrary arrays of wind turbines*
[36] Crespo A, Hernández J and Frandsen S 1999 *Wind Energy* **2** 1–24
[37] Katić I, Højstrup J and Jensen N 1987 A simple model for cluster efficiency
[38] Troldborg N and Meyer Forsting A R 2017 *Wind Energy* **20** 2011–2020
[39] Schøler J P, Réthoré P E, León J P M, Riva R, van der Laan P and Risco J C 2023, forthcoming